

Regulation of membrane scission in yeast endocytosis

Deepikaa Menon¹ and Marko Kaksonen^{1*}

*For correspondence:

Marko.Kaksonen@unige.ch ()

¹Department of Biochemistry, University of Geneva, Geneva, Switzerland

Abstract

Introduction

In Clathrin-mediated endocytosis, a flat plasma membrane is pulled into a tubular invagination that eventually forms a vesicle. Forces that drive the transition from invagination to spherical vesicle in mammalian cells are provided by constriction of the GTPase Dynamin. Dynamin is now known to act in concert with the crescent-shaped N-BAR proteins Endophilin and Amphiphysin (ref. Dynamin papers). Proline-rich motifs on the Dynamin. In yeast cells, what causes membrane scission is unclear, although the yeast N-BAR protein complex Rvs has been identified as an important component of the scission module. In yeast, the Amphiphysin and Endophilin homologue Rvs is a heterodimeric complex composed of Rvs161 and Rvs167 (Friesen et al., 2006). Deletion of Rvs reduces scission efficiency by nearly 30% and reduces the invagination lengths at which scission occurs (ref Marko, wanda). Apart from a canonical N-BAR domain which forms a crescent-shaped structure, Rvs167 has a Glycine-Proline-Alanine rich (GPA) region and a C-terminal SH3 domain. Rvs161 and Rvs167 N-BAR domains are 42% similar, and 21% identical, but are not interchangeable (Sivadon, Crouzet and Aigle, 1997). The GPA region is thought to act as a linker with no known other function, while loss of the SH3 domain affects budding pattern and actin morphology. Most Rvs deletion phenotypes can however, be rescued by expression of the BAR domain alone (Sivadon, Crouzet and Aigle, 1997), suggesting that the BAR domains are the main functional unit of the Rvs complex. Homology modelling has shown that the BAR domain of Rvs167 is similar to Amphiphysin and Endophilin (Youn et al., 2010), and is therefore likely to function similarly to the mammalian homologues. In keeping with this theory, Rvs has been shown to tubulate liposomes in vitro (Youn et al., 2010). The Rvs complex arrives at endocytic sites in the last stage of the endocytosis, and disassembles rapidly at the time of membrane scission (Picco et al., 2015), consistent with a role in membrane scission. While it is known to be involved in the last stages of endocytosis, a mechanistic understanding of the influence of Rvs on scission however, remains incomplete. u89

We used quantitative live-cell imaging and genetic manipulation in *S.cerevisiae* to investigate the influence of Rvs and several Rvs interacting proteins that have been suggested to have a role in scission. We found that arrival of Rvs to endocytic sites is timed by interaction of its BAR domain with a specific membrane curvature. The Rvs167 SH3 domain affects localization efficiency of the Rvs complex and also influences invagination dynamics. This indicates that both BAR and SH3 domains are important for the role of Rvs as a regulator of scission. We tested current models of membrane scission, and find that deleting yeast synaptojanins or dynamin does not change scission dynamics. Interfacial forces at lipid boundaries are therefore unlikely to be sufficient for scission, and forces exerted by dynamin are not required. Furthermore, invagination length is insensitive to overexpression of Rvs, suggesting that the recently proposed mechanism of BAR-induced protein friction on the membrane is not likely to drive scission. We propose that recruitment of Rvs BAR

domains prevents scission and allows invaginations to grow by stabilizing them. We also propose that vesicle formation is dependent on forces exerted by a different module of the endocytic pathway, the actin network. Preventing premature membrane scission via BAR interaction could allow invaginations to grow to a particular length and accumulate enough forces within the actin network to reliably cut the membrane.

Results

Removal of Rvs167, not Vps1, results in reduced coat movement

Yeast Dynamin-like protein Vps1 does not contain the canonical Proline Rich Domain, which in mammalian cells is required for recruitment to endocytic sites (ref Grabs et al., 1997; Cestra et al., 1999; Farsad et al., 2001; Meinecke et al., 2013). Some work has reported its recruitment at endocytic proteins (ref Ayscough, Yu, 2004; Nannapaneni et al., 2010). Vps1 tagged both N- and C-terminally with GFP constructs failed to co-localize with endocytic protein Abp1 in our hands (Fig.1 supplement), consistent with other work that observed localization only with other parts of the trafficking pathway (ref Gadila 2017).

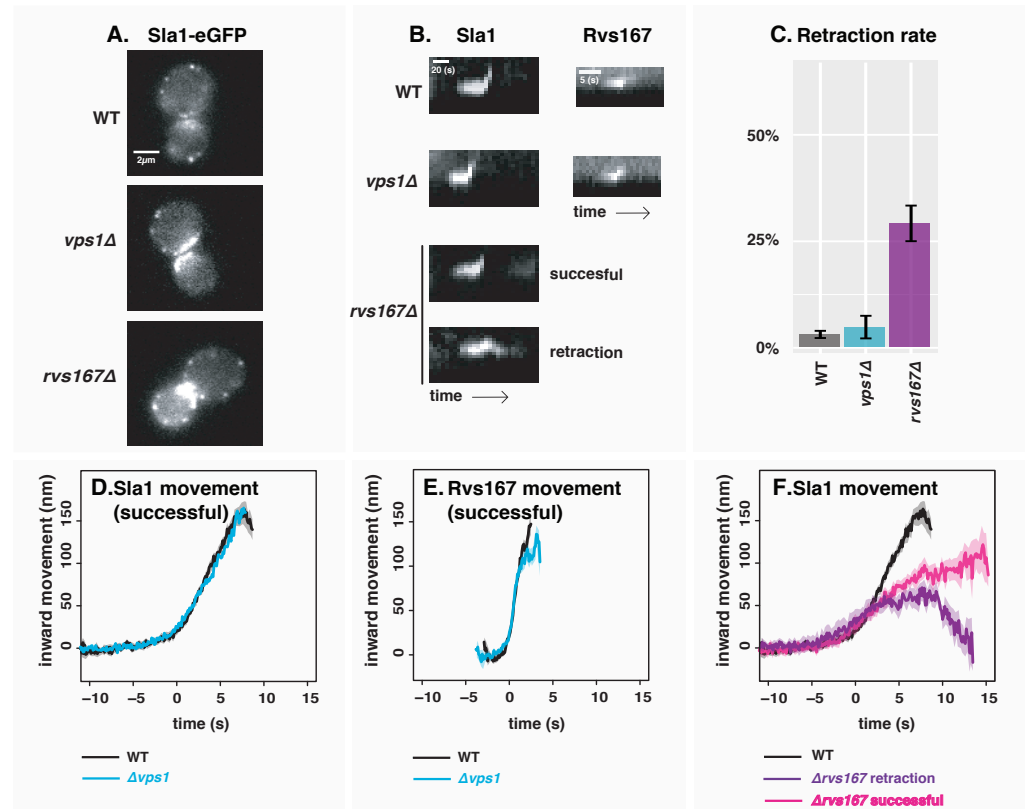


Figure 1. *vps1Δ* and *rvs167Δ* deletion **A:** Slice from image of WT, *vps1Δ*, and *rvs167Δ* cells expressing Sla1-eGFP. Scale bar= 2μm. **B:** Representative kymographs of Sla1-eGFP and Rvs167-eGFP patches in WT, *vps1Δ*, and *rvs167Δ* cells. Scale bar for Sla1-egfp = 20(s), scale bar for Rvs167-eGFP = 5(s). **C:** Histogram of Sla1-eGFP retraction percentages in WT, *vps1Δ*, and *rvs167Δ* cells. Error bars are standard deviation from two data sets, $p < 0.001 = *$. **D:** Averaged centroid positions of Sla1-eGFP in WT and *vps1Δ* cells. **E:** Averaged position of Rvs167-eGFP in WT and *vps1Δ* cells. **F:** Averaged position of Sla1-eGFP in WT, and successful and retracted Sla1-eGFP positions in *rvs167Δ* cells. All averaged positions are aligned in time to begin inward movement at the same time=0(s), and aligned in space to a starting position = 0(nm). Note that in E, averaged Rvs167-eGFP inward movement is concomitant with the maxima of its fluorescent intensity (Fig1.supplement3)

To test whether absence of Vps1 influences scission, dynamics of endocytosis are observed in

58 cells lacking Vps1 and compared against wild-type (WT) cells (Fig.1A-F). Vps1 deletion is confirmed
59 by sequencing the open reading frame, and these cells show a growth phenotype at 37°C (Fig.1,
60 supplement2) that has been previously reported (ref. ayscough). Rates of retraction of the mem-
61 brane in *vps1Δ* and WT cells is quantified by tracking the endocytic coat protein Sla1 tagged at
62 the C-terminus with eGFP (Fig.1C). Upon actin polymerization, the endocytic coat is pulled into
63 the cytoplasm along with the membrane as it invaginates (ref.Skruczny?). Coat protein Sla1 thus
64 acts as a proxy for the behaviour of the plasma membrane. Membrane retraction, that is, inward
65 movement and subsequent retraction of the invaginated membrane back towards the cell wall is a
66 scission-specific phenotype (ref.Marko). Retraction rates do not increase in *vps1Δ* cells compared to
67 the WT (Fig.1C).

68
69
70 In order to study the total inward movement of the endocytic coat, and therefore the depth of
71 the endocytic invagination, the averaged centroid trajectory of 50 Sla1-eGFP patches (ref. Picco,
72 eLife 2015) in *vps1Δ* and WT cells is tracked and compared (Fig.1D). In brief: yeast cells expressing
73 fluorescently-tagged endocytic proteins are imaged at the equatorial plane. Since membrane
74 invagination progresses perpendicularly to the plane of the plasma membrane, proteins that move
75 into the cytoplasm during invagination do so in the imaging plane. Centroids of Sla1 patches- each
76 patch being an endocytic site- are tracked in time and averaged. This provides an average centroid
77 that can be followed with high spatial and temporal precision. For more details, refer to Picco et. al,
78 eLIFE 2015. Averaged centroid movement of Sla1-eGFP in WT cells is linear to about 140nm (Fig.1D).
79 Sla1 movement in *vps1Δ* cells has the same magnitude of movement (Fig.1D). In spite of slight
80 differences in the rates of movement, the total inward movement- and so the depth of endocytic
81 invagination- does not change.

82
83
84 Centroid tracking has shown that the number of molecules of Rvs167 peaks at the time of
85 scission, and is followed by a rapid loss of fluorescent intensity, simultaneous with a sharp jump
86 of the centroid into the cytoplasm (ref.Andrea). This jump, also seen in Rvs167-GFP kymographs
87 (Fig.1B), is interpreted as loss of protein on the membrane tube, causing an apparent spatial jump
88 to the protein localized at the base of the newly formed vesicle. Kymographs of Rvs167-GFP (Fig.1B),
89 as well as Rvs167 centroid tracking (Fig.1E) in Vps1 deleted cells show the same jump as in WT.

90
91
92 Since removal of the Rvs complex is known to increase the membrane retraction rate at endocytic
93 sites (ref Marko), involvement of the Rvs proteins in the scission process was investigated further.
94 The Rvs complex is composed of Rvs161 and Rvs167 dimers (ref.Dominik), so deletion of Rvs167
95 effectively removes both proteins from endocytic sites. We quantified the effect of *rvs167Δ* on
96 membrane invagination (Fig.1A-C). 27% of Sla1 patches move inward and then retract in *rvs167Δ*
97 cells (Fig.1C). Similar retraction rates were measured in other experiments (Kaksonen, Toret and
98 Drubin, 2005), and suggest failed scission in these 27% of endocytic events. Coat movement both of
99 retractions and of successful endocytic events were quantified (Fig.1F) as described in Picco et. al,
100 2015. Sla1 centroid movement in both successful and retracting endocytic events in *rvs167Δ* cells
101 look similar to WT up to about 50nm (Fig.1F). In WT cells, Abp1 intensity begins to drop at scission
102 time; similarly, in successful endocytic events, Abp1 intensity drops after Sla1 centroid has moved
103 about 100nm (Fig.1supplement), suggesting that scission occurs at invagination lengths between 60
104 -100 nm. That membrane scission occurs at shorter invagination lengths than in WT is corroborated
105 by the smaller vesicles formed in *rvs167Δ* cells by Correlative light and electron microscopy (CLEM)
106 (Kukulski et al., 2012). CLEM has moreover shown that Rvs167 localizes to endocytic sites after
107 the invaginations are about 60nm long (Kukulski et al., 2012). Sla1 movement in *rvs167Δ* indicates
108 therefore that membrane invagination is unaffected till Rvs is supposed to arrive. The Sla1 centroid

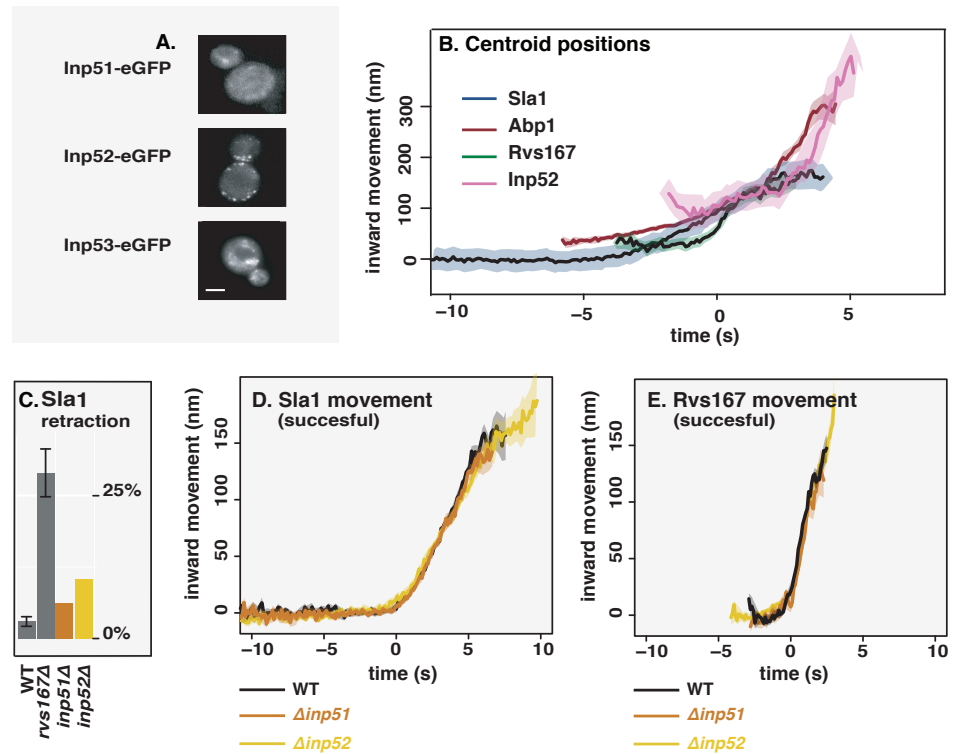


Figure 2. Involvement of yeast Synaptojanin-like proteins in endocytosis A. Cells with endogenously tagged Inp51, Inp52, and Inp53. B. Inp52 centroid trajectory is aligned in space and time to other endocytic proteins. C: Sla1 retraction rates in *inp51Δ* and *inp52Δ* cells compared to WT and *rvs167Δ*. Error bars are standard deviation from two data sets. D: Averaged centroid positions of Sla1-eGFP in WT, *inp51Δ*, and *inp52Δ* cells. E: Averaged centroid positions of Rvs167-eGFP in WT, *inp51Δ*, and *inp52Δ* cells.

for retraction events moves back towards its original position after inward movement.

Synaptojanins likely influence vesicle uncoating, but not scission dynamics.

Three Synaptojanin-like proteins have been identified in budding yeast: Inp51, Inp52, and Inp53. Inp51-eGFP exhibits a diffuse cytoplasmic signal, Inp52-eGFP localizes to cortical actin patches that are endocytic sites (Fig2 supplement) and Inp53 localizes to patches within the cytoplasm (ref). Spatial and temporal alignment of Inp52 with Sla1, Abp1, and Rvs167 (ref.Pico) shows that Inp52 protein molecules arrive in the late stage of endocytosis after Rvs167, and localizes to the invagination tip, suggesting a potential role in membrane scission (Fig.2b).

Inp53 was not investigated further, as its localisation conforms with other literature that find it is involved in the golgi trafficking pathway rather than endocytosis (ref Golgi). Although we were unable to see Inp51 localisation at endocytic sites, it may be recruited in small numbers below our detection limit. Deletion of Inp51 has been shown to exacerbate the effect of *inp52Δ* on membrane retraction (ref Liu), so both Inp51 and Inp52 were tested as potential candidates as scission regulators.

Dynamics of Sla1-eGFP and Rvs167-eGFP in either *inp51Δ* or *inp52Δ* cells were compared against the WT. Membrane retraction events do not significantly increase in either compared to the WT (Fig2c).

Magnitude and speed of Sla1 and Rvs167 centroid movement in *inp51Δ* is the same as the WT (Fig2.d, e). In *inp52Δ* cells, Sla1 movement also has the magnitude and speed as WT, but Sla1-eGFP signal is persistent after membrane scission (Fig.2d, arrow). Similarly, although Rvs167 inward

130 movement looks similar to WT in *inp52Δ* (Fig2e), Rvs167-eGFP signal is persistent after inward
 131 movement (Fig2e arrow), and Rvs167 and Sla1 disassembly has a delay (Fig2 supplement)

132 **Rvs BAR domains recognize membrane curvature in-vivo**

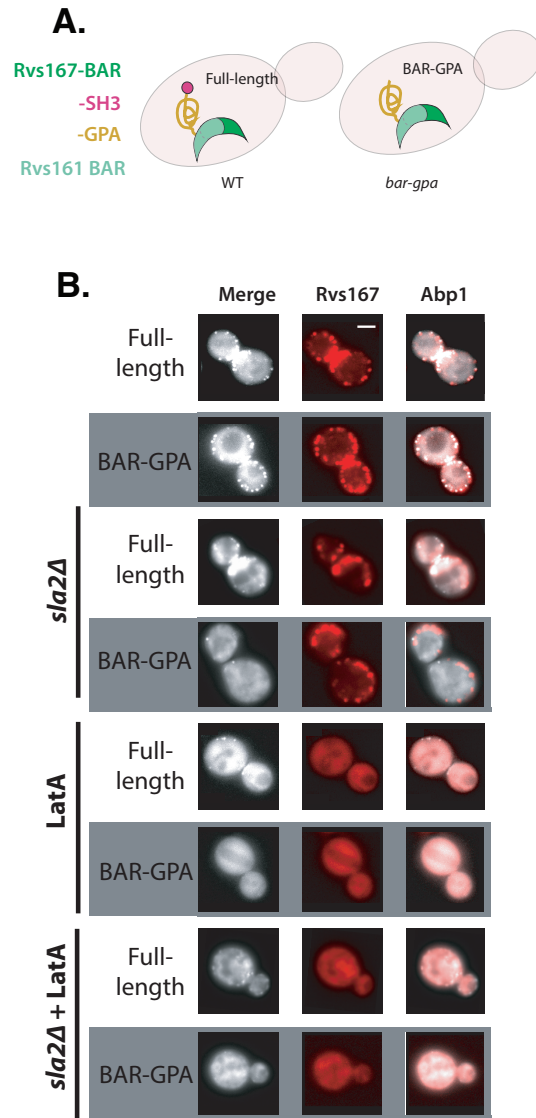


Figure 3. Localization of Rvs167 BAR domain A: Schematic of Rvs protein complex with and without the SH3 domain. B: Localization of full-length and BAR-GPA in WT, *sla2Δ*, LatA treated, and LatA treated *sla2Δ* cells. C: Localization of full-length Rvs167-eGFP in WT, *myo3Δ*, *myo5Δ*, and *vrp1Δ* cells. Scale bars=2μm.

133 So far Rvs167 remains the protein that has a major influence on scission rates and inward
 134 moment of Sla1. Recruitment of the Rvs complex to endocytic sites was thus investigated further.
 135 Interaction between Rvs and membrane curvature in vivo has been indicated by work on other BAR
 136 domain proteins (ref BAR), but has not so far been tested. In order to do so, we deleted the SH3
 137 domain of Rvs167 leaving the N-terminal BAR and GPA regions (henceforth BAR-GPA, Fig3a) and
 138 observed the localization of the BAR region without SH3 influence. The GPA region is a disordered
 139 domain that has no previously reported function (ref) and was retained to ensure proper folding and
 140 function of the BAR domain. Endogenously tagged Rvs167-eGFP and BAR-GPA-eGFP colocalization

141 with Abp1-mCherry in WT and *sla2Δ* cells were compared (Fig3b). Sla2 acts as the molecular linker
 142 between forces exerted by the actin network and the plasma membrane (ref. Skruzny). *sla2Δ* cells
 143 therefore contain a polymerizing actin network at endocytic patches, but the membrane has no
 144 curvature, and endocytosis fails. In these cells, the full-length Rvs167 protein co-localizes with
 145 Abp1-mCherry, indicating that it is recruited to endocytic sites (Fig3b, "*sla2Δ*"). BAR-GPA localization
 146 is removed, except for rare transient patches that do not co-localize with Abp1-mCherry.

147 **Rvs SH3 domains have an actin and curvature independent localisation**

148 The SH3 domain has known genetic interactions with actin-related endocytic proteins. In order to
 149 test if these interactions are prevalent in vivo, we tested the localisation of full-length Rvs167 and
 150 BAR-GPA in LatA treated cells (Fig3b, "LatA"). Plasma membrane localisation of full-length Rvs167
 151 remains upon LatA treatment, and transient patches continue to exist in *sla2Δ* cells treated with
 152 LatA (Fig3b, "*sla2Δ*+ LatA"). BAR-GPA localisation on the other hand, is removed in both.

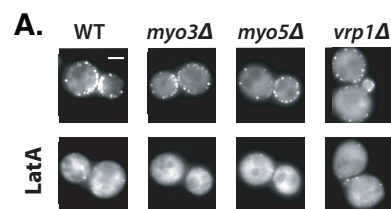


Figure 4. Localization of the SH3 domain A: Schematic of Rvs protein complex with and without the SH3 domain, roughly based on homology models with Amphyphisin and Endophylin. B: Localization of full-length and BAR-GPA in WT, *sla2Δ*, LatA treated, and LatA treated *sla2Δ* cells. C: Localization of full-length Rvs167-eGFP in WT, *myo3Δ*, *myo5Δ*, and *vrp1Δ* cells. Scale bars=2μm.

153 **SH3 domains are likely recruited by Myosin 3**

154 Type I myosins Myo3 and Myo5, and Vrp1 have genetic or physical interactions with Rvs167 SH3
 155 domains (Lila and Drubin, 1997; Colwill et al., 1999; Madania et al., 1999; Liu et al., 2009). We tested
 156 the interaction between these proteins and the Rvs167 SH3 region by studying the localization
 157 of full-length Rvs167 in cells with one of these proteins deleted, and treated with LatA. By LatA
 158 treatment we expected to produce the situation in which BAR-curvature interaction is removed
 159 (Fig3b). Then if we lost SH3 interaction because we deleted the protein with which it interacts, we
 160 would lose localisation of Rvs167 completely. Deletion of neither Vrp1 nor Myo5 in combination
 161 with LatA treatment removes the localization of Rvs167. Deletion of Myo3 with LatA treatment
 162 removes localization of Rvs167.

163 **what about the differences in myo5 and myo3 number...**

164 **Loss of Rvs167 SH3 domain affects coat and actin dynamics**

165 Since the Rvs167 SH3 domain appears to have an important influence on the recruitment of the
 166 Rvs complex to endocytic sites, we wondered if the domain also had an influence on endocytic
 167 dynamics. We compared dynamics of Sla1 and Rvs167 in WT and BAR-GPA strains (Fig4). Movement
 168 of Sla1 centroid is slower in BAR-GPA cells than in WT (Fig4a). Tubular invaginations are formed
 169 in BAR-GPA cells, and qualitatively resemble those in WT, as seen by CLEM (Fig.4 supplement).
 170 Recruitment of both Rvs167 and Abp1 molecules is delayed in BAR-GPA cells. However, Rvs167
 171 centroids in both WT and BAR-GPA arrive at endocytic sites when the Sla1 centroid is 20-30 nm
 172 away from its starting position. BAR-GPA accumulation also begins when Abp1 molecule numbers
 173 in the mutant are about the same as in WT (about 300 copies, Fig4b). Taken together, this data
 174 suggests that the Rvs complex is recruited to a specific geometry of membrane invagination, and

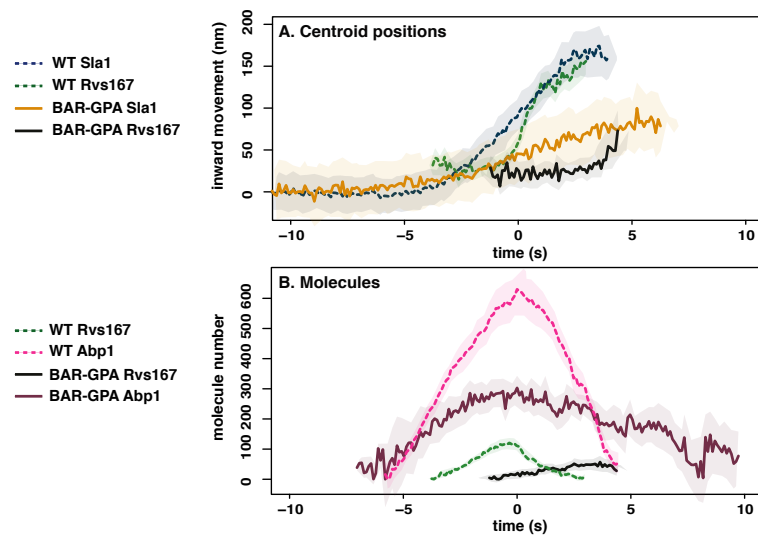


Figure 5. Endocytic dynamics in BAR-GPA cells A: Averaged centroid positions of Sla1 and Rvs167 aligned in space and time so that time=0(s) is the peak of fluorescent intensity of Abp1 in WT and BAR-GFP strains. B: Numbers of molecules of in WT and BAR-GPA strains, aligned so that time=0(s) is the maximum of fluorescent intensity of Abp1 in the corresponding strains.

that Rvs167 recruitment in BAR-GPA is delayed because invaginations in this mutant take longer to acquire this specific geometry.

The inward jump of Rvs167 is smaller in BAR-GPA cells than in WT (Fig.4b), consistent with the formation of shorter invaginations suggested by the reduced Sla1 movement in these cells. Recruitment of Rvs167 in BAR-GPA cells is reduced to half of that in WT (Fig4b), although cytoplasmic concentration of Rvs167 in both cell types are not different (Fig4 supplement). Recruitment therefore is unlikely to be limited by cytoplasmic expression of the mutant protein. Abp1 disassembly is slowed down in BAR-GPA cells compared to WT, and recruitment is reduced to 50% of WT recruitment (Fig.4b), likely indication disruption of actin network dynamics.

Increased BAR domain recruitment corresponds to increased membrane movement

We wondered if the decreased Sla1 movement in BAR-GPA cells (Fig4a) was induced by loss of an SH3 domain mediated interaction, or because Rvs167 in the BAR-GPA mutant is recruited in smaller numbers to endocytic sites. To check whether increasing the recruitment of the Rvs complex can rescue reduced Sla1 movement, Rvs167 and Rvs161 genes were duplicated endogenously (ref Huber) in diploid and haploid yeast cells. In haploid cells, increasing the number of Rvs167 and Rvs161 genes results in increased recruitment of Rvs167 to about 1.6 times the WT amount (Fig5c). Sla1 dynamics remains the same as in the WT (Fig5a). Duplicating the BAR-GPA domain alone increases the amount of BAR-GPA molecules recruited to endocytic sites (Fig5c), and rescues the loss of Sla1 movement in the 1x BAR-GPA, as well the inward jump of BAR-GPA itself (Fig5a,b). By gene duplication, diploid cells are generated containing either 4 copies of both Rvs genes, 2 copies of each gene (WT diploid), or 1 copy (by deleting one copy of Rvs167 and Rvs161). In diploid cells (Fig5d-f), amount of Rvs167 recruited to sites increases with gene copy number (Fig5f). Adding excess Rvs to endocytic sites in the 4x case does not change the rate or total inward movement of Sla1, or of Rvs167 (Fig5d,e). In the case of 1x Rvs, Sla1 movement is slightly reduced after 100nm (Fig5a). Magnitude of Rvs167 inward movement is unchanged, but the Rvs167-eGFP signal is lost immediately after the inward movement, unlike in the 4x and 2x cases. We measured the total number of Abp1 molecules at endocytic sites for different strains (Fig5g,h), and found that higher Abp1 numbers corresponds to larger Sla1 centroid movement. Total Abp1 numbers recruited are

reduced for 1xBAR and *rvs167* Δ strains (Fig5g,h), suggesting a correlation between the maximum number of Abp1 recruited and total invagination length.

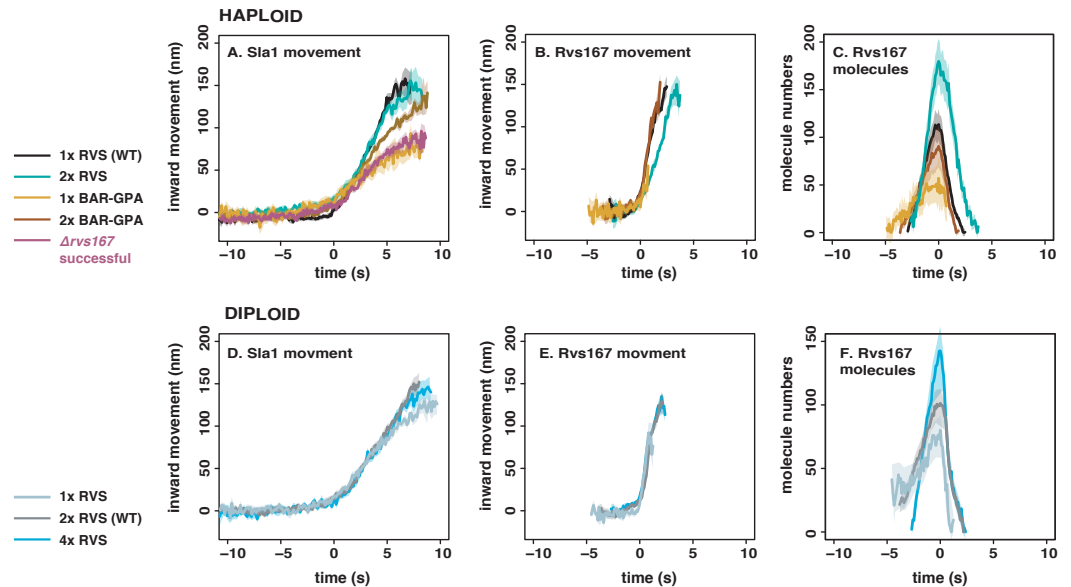


Figure 6. RVS duplication in haploid and diploid cells A: Sla1 centroid positions in haploid strains with different numbers of copies of Rvs167 and Rvs161 genes. B: Rvs167 centroid positions. C: Recruitment of Rvs167 in time in these strains. D: Sla1 centroid positions in diploid strains expressing different numbers of copies of Rvs167 and Rvs161. E, F: Rvs167 centroid positions, and recruitment in time, in the diploid strains. All centroid positions are aligned in the time axis so that time=0(s) corresponds to beginning of inward movement of the average centroid for each corresponding strain. They are aligned in the y axis so that y=0(nm) corresponds to the beginning of the average centroid position

Discussion

Recruitment and function of the Rvs complex in has been explored in this work, as well as several models for how membrane scission could be effected in yeast endocytosis. We propose that Rvs is recruited to endocytic sites by interactions between the Rvs BAR domains and invaginated membrane, and that SH3 domain mediated protein-protein interactions are required for efficient recruitment of Rvs to sites. Arrival of Rvs on membrane tube scaffolds the membrane and prevents premature membrane scission. Effective scaffolding depends on recruitment of a critical number of Rvs molecules. Rvs is a relatively short-lived protein at endocytic sites. It is recruited only once membrane tube is formed (Kaksonen, Toret and Drubin, 2005; Kukulski et al., 2012; Picco et al., 2015). FCS measurements (Boeke et al., 2014) have shown that the cytosolic concentrations of Rvs167 and Rvs161 are high (354nM and 721nM respectively) compared to other endocytic proteins like Las17, Vrp1, Myo3, and Myo5 (80-240nM). In spite of this, relatively few numbers of Rvs are recruited to endocytic sites, suggesting that recruitment is tightly regulated. In the case of Rvs, both timing and efficiency appear crucial to its function, the question is what confers both.

BAR domains sense *in vivo* membrane curvature and time recruitment of Rvs

The curved structure of BAR dimers (Peter et al., 2004; Mim et al., 2012) has suggested that Rvs is recruited by its preference for some membrane shapes over others, supported by its arrival at curved membrane tubes. In the absence of membrane curvature, in *sla2* Δ cells, the BAR domain alone does not localize to cortical patches (Fig.3b,c). This demonstrates for the first time that the BAR domain does indeed sense and requires membrane curvature to localize to cortical patches. Work on BAR domains have proposed that electrostatic interactions at the concave surface and

tips of the BAR domain structure mediate membrane binding (Qualmann, Koch and Kessels, 2011). Mutations in these lipid-binding surfaces would clarify the interaction with underlying lipids, and test if Rvs relies on similar interactions. BAR is able to localize to endocytic sites, and has a similar lifetime in WT cells (Fig4b). However, time alignment with Abp1 shows that there is a delay in the recruitment of BAR-GPA compared to Abp1 arrival, compared to full-length Rvd167 (Fig4c). The delayed recruitment occurs because the invagination takes longer to reach a particular length: Sla1 moves inwards at a slower rate in BAR cells, and it takes longer for the membrane in BAR-GPA cells to reach the same length as Rvs167. Rvs167 arrives in BAR cells when Sla1 has moved inwards 25-30nm (dashed red lines in Fig.4a), which is also the distance Sla1 has moved when Rvs167 arrives in WT. By the time Sla1 has moved this distance, the membrane is already tubular (Kukulski et al., 2012; Picco et al., 2015), consistent with Rvs arrival at invaginated tubes. This suggests Rvs recruitment is timed to specific membrane invagination length- therefore to a specific membrane curvature- and that this timing is provided by the BAR domain.

SH3 domains allow efficient and actin independent recruitment

Rvs167 in BAR cells accumulates to about half the WT number (Fig.3c), even though the same cytoplasmic concentration is measured (supplement Fig3?), indicating that the SH3 domain increases the efficiency of recruitment of Rvs. In *sla2Δ* cells, full-length Rvs can assemble on the membrane (Fig.3b,c). Since BAR domains alone do not localize to patches in *sla2Δ* cells, full-length localization must be mediated by the SH3 domain, supporting a role for the SH3 domain in increasing recruitment of Rvs by clustering protein molecules. That full-length Rvs167 is able to assemble and disassemble at cortical patches in *sla2Δ* cells without the curvature- dependent interaction of the BAR domain (Fig.3b,c) indicates that the SH3 domain is able to mediate both the recruitment and the disassembly of Rvs at the endocytic site. In *sla2Δ* cells treated with LatA (Fig.3c), actin-based membrane curvature is inhibited, and the actin patch proteins are removed from the plasma membrane. Full-length Rvs167 in these cells still shows transient localizations at the plasma membrane. In *sla2Δ* cells treated with LatA, the localization of BAR is lost. This suggests that localization of the full-length Rvs167 in LatA treated cells is dependent on an SH3 domain interaction, and that this is independent of both actin and membrane curvature.

In WT cells, the Abp1 and Rvs167 fluorescent intensities reach maxima concomitantly (Fig4b), and the consequent decay of both also coincide. Coincident disassembly indicates that upon vesicle scission, the actin network is immediately disassembled. Membrane scission essentially occurs around the intensity peak of the two proteins. This coincident peak is lost in BAR-GPA cells: BAR-GPA-eGFP in these cells peaks several seconds after Abp1 intensity starts to drop, and the decay of Abp1 is prolonged, taking nearly double the time as in WT. The number of Abp1 molecules recruited is decreased to about two thirds the WT number. Although it is not clear what the decoupling of Abp1 and Rvs peaks means, the changes in Abp1 dynamics suggests a strong disruption of the actin network dynamics. SH3 domains are known to interact with components of the actin network like Abp1 and Las17 (Lila and Drubin, 1997; Madania et al., 1999), but study of other components of the actin machinery will be required to understand how exactly loss of the SH3 has changed the progression of endocytosis.

SH3 interaction with an endocytic binding partner likely help recruit Rvs to endocytic sites. Many such interaction partners have been proposed. Abp1 interaction with the Rvs167 SH3 domain has been shown (Lila and Drubin, 1997; Colwill et al., 1999), as has one with WASP protein Las17 (Madania et al., 1999; Liu et al., 2009), yeast Calmodulin Cmd1 (Myers et al., 2016), type I myosins (Geli et al., 2000), and Vrp1 (Lila and Drubin, 1997). All of these suggested binding partners localize to the base of the invagination (Yidi Sun, 2006; Picco et al., 2015), and do not follow the invaginating membrane into the cytoplasm. The SH3 interaction partner is likely Myo3 (Fig3d), and SH3 domains interact with the endocytic network at the base of the invagination. Centroid tracking however, suggests that Rvs is accumulated all over the membrane tube. If Rvs was recruited to the base and pulled up as the invagination grows, the centroid would move continuously upwards rather than

277 remain relatively non-motile before the jump at scission time. It is possible that the SH3 initially
278 helps cluster near the base, and as the membrane invaginations grow longer, BAR-membrane
279 interactions dominate.

280 **Accumulation of Rvs on membrane invagination**

281 When ploidy is doubled from haploid to diploid yeast cells, we could expect that double the protein
282 amount is expressed and recruited, but it does not appear so. The amount of Rvs recruited in
283 WT haploid and diploids remains about the same, and cytoplasmic signal is similar (Fig.5, Fig5
284 supplement). This invariance between accumulated protein in haploids and diploids shows that Rvs
285 recruitment is not determined by the number of alleles of Rvs. Haploid and diploid cells appear
286 to tune the amount of Rvs recruitment to get a specific amount to endocytic sites. WT diploids
287 (2xd) contain two copies each of RVS161 and RVS167 genes. Rvs duplicated diploids, which contain
288 four copies each of RVS167 and RVS161 (4xd) could be expected to express and recruit to sites
289 twice the amount of Rvs as 2xd. However, compared to 2xd, cytoplasmic signal in 4xd increases
290 by 1.6x and recruitment of Rvs167 to endocytic sites increases only by 1.4x. Doubling the gene
291 copy number increases, but does not double protein expression or recruitment in the case of
292 Rvs. Similarly, duplicating Rvs genes in haploid cells results in an increase in number of molecules
293 recruited, but not in doubling (1xh, 2xh). Although the rate of adding Rvs is different in haploids and
294 diploids, in both cases, it increases by gene copy number (yellow line in Fig.4.2). Cytoplasmic protein
295 concentration is increased when gene copy number is increased, and recruitment to endocytic
296 sites is increased by the increase in cytoplasmic concentration. These data suggest that the amount
297 of Rvs that is recruited scales with available concentration of protein. Comparing across ploidy
298 however, the rate of Rvs recruitment is lower in WT diploid compared to WT haploid (2xd vs 1xh,
299 Fig.4.1)

300 for this is not clear. 4.2 Arrangement of Rvs dimers on the membrane A homology model of
301 the Rvs BAR dimer structure based on Am- phiphysin suggests that it has the concave structure
302 typical for N- BAR domains. Rvs is a hetero- rather than homodimer unlike Am- phiphysin, and a
303 high-resolution structure will be necessary to clarify the interaction and arrangement of Rvs on
304 endocytic tubes. There are some indications from the experiments in this thesis however, regarding
305 its interaction with the membrane. 4.2.1 Rvs does not form a tight scaffold on membrane tubes
306 Observations of in vitro helices of BAR domains have suggested that Rvs might form a similar helical
307 scaffold. The number of Rvs molecules recruited to endocytic sites is high enough to cover the
308 surface area of the tubular invagination, so it has been proposed that an Rvs scaffold covers the
309 entire membrane tube up to the base of the future vesicle (Picco et al., 2015). In Rvs duplicated
310 diploid cells (4xd), Rvs can be recruited at a much faster rate than in the WT (2xd) (Fig.3.10B-
311 C, Fig.4.2) while disassembly dynamics is the same in both (Fig.3.10C, Fig.4.3). The exponential
312 decay of fluorescent intensity in WT haploid and diploid cells (1xh, 2xd, Fig.4.3) indicates that
313 all of the protein is suddenly disassembled from the endocytic site. When the membrane tube
314 undergoes scission, there is no more tubular curvature for the Rvs to bind to. The sharp decay is
315 therefore consistent with a BAR scaffold that breaks upon vesicle scission because there is no more
316 membrane interaction, releasing all the membrane-bound protein at once. A similar decay in the
317 4xd strain suggests that all the Rvs in this case is also bound to the membrane: if the protein was
318 not bound to the membrane, fluorescent intensity would not decay sharply. Since the membrane is
319 able to accommodate 1.4x the amount of BAR protein as the WT, it would suggest that at lower
320 protein amounts, a tight helix that covers the entire tube is not likely. Adding molecules to a tube
321 already completely covered by a scaffold would result in a change in Rvs assembly and disassembly
322 dynamics. Further, additional molecules would have to be added at the top or base of a tight
323 scaffold. At the top, the radius of curvature is decreased compared to the tube since this is the
324 rounded vesicle region. At the base, the plasma membrane is nearly flat, and the Rvs BAR domain
325 is similarly unlikely to favour interactions here. Otherwise the scaffold would have to be disrupted
326 to add new molecules, which would likely slow down recruitment rate rather than speed it up.

327 Molecules could also be added concentric to an existing scaffold. However, the concave surface of
 328 Rvs is known to interact with lipids, and multiple layers of BAR domains on the membrane tube
 329 would probably not show the sudden disassembly seen here. I assume that the membrane surface
 330 area does not change in the 4xd compared to 2xd from the identical movement of Sla1 in both
 331 cases (Fig.3.10A). It is possible that a wider tube is formed, which would increase the membrane
 332 surface area for BAR binding. This would, however, require the BAR domains to interact with a lower
 333 radius of curvature than in WT. This seems unlikely, and in the absence of any indication otherwise,
 334 I assume that the membrane tubes in all diploid and haploid cases have the same width. 4.2.2 A
 335 limit for how much Rvs can be recruited to the membrane In the case of Rvs duplication in haploids
 336 (2xh), a change in disassembly dynamics is seen (Fig.3.9C, Fig.4.3). In 2xh, the maximum number
 337 of molecules recruited is 178 ± 7.5 compared to the maximum of 113.505 ± 5.2 in WT (1xh). This is
 338 means that nearly 1.6x the WT amount of protein is recruited to membrane tubes in in the 2xh case.
 339 The Rvs167 fluorescent intensity in 2xh shows a delay in disassembly. This suggests that the excess
 340 protein may not be directly on the membrane, since if the protein was membrane bound, when the
 341 membrane breaks, the protein must be released. The excess Rvs could either interact with the actin
 342 network via the SH3 domain, or interact with other Rvs dimers. By a similar argument as in 4.2.1
 343 above, I do not expect that multiple layers of BAR domains are formed, and that the excess protein
 344 is recruited by the interaction of the SH3 domain. Another explanation for the delayed disassembly
 345 is that at high concentrations of Rvs like in the 2xh case, a tight BAR scaffold is formed, and the
 346 BAR domains interact with adjacent BAR domains. When the membrane undergoes scission, the
 347 protein is no longer membrane-bound, but lateral interactions delay disassembly of the scaffold.
 348 Lateral interactions between neighbouring BAR dimers have been shown in the case of Endophilin
 349 (Mim et al., 2012). It is not currently clear where the Rvs molecules are added in the 2xh case:
 350 superresolution microscopy could clarify whether it is added at the membrane tube. Whatever
 351 the arrangement of the Rvs complex on the membrane, disassembly dynamics is changed in the
 352 case of 2xh, compared to the other haploid and diploid strains. Since the number of Rvs molecules
 353 is highest in this strain, this suggests that there is a limit to how much Rvs can assemble on the
 354 tube without altering interaction with the endocytic protein network. 4.2.3 Conclusions for Rvs
 355 localization All of these data support the idea that Rvs recruitment rate and total numbers are
 356 determined by concentration of protein in the cell. The maximum number of molecules that can
 357 interact with the membrane is limited by the surface area of the invagination. Although more can
 358 be recruited, Rvs molecules over a certain threshold interact in a different way with endocytic sites,
 359 possibly via the SH3 domain. Timing of recruitment to sites is by curvature-recognition via the BAR
 360 domain, while efficiency of recruitment and interaction with the actin network is established via the
 361 SH3 domain. 4.3 What causes membrane scission?

362 **Rvs acts as a membrane scaffold preventing membrane scission**

363 Invaginations in *rvs167Δ* cells undergo scission at short invagination lengths of about 80nm (Fig.3.2),
 364 compared to the WT lengths of 140nm. This shows that first, enough forces are generated at
 365 80nm to cause scission. Then, that Rvs167 is required at membrane tubes to prevent premature
 366 scission. Prevention of scission at short invagination lengths can be explained by Rvs stabilizing
 367 the membrane invagination via membrane interactions of the BAR domain (Boucrot et al., 2012;
 368 Dmitrieff and Nedelec, 2015). Rvs preventing membrane scission could also be explained by the
 369 SH3 domain mediating actin forces to the invagination neck: one can imagine that the SH3 domain
 370 somehow decouples actin forces from the neck, and that this delays scission. Since invagination
 371 lengths of *rvs167a* cells are increased towards WT by overexpression of the BAR domain alone
 372 (Fig.3.12A), I propose that localization of Rvs BAR domains to the membrane tube stabilizes the
 373 membrane. This allows deep invaginations to grow until actin polymerization produces enough
 374 forces to overcome this stabilization and sever the membrane. Stabilization of the membrane
 375 tube increases with increasing amounts of BAR domains recruited to the membrane tube (Fig.3.12).
 376 The requirement for Rvs scaffolding cannot be removed by reducing turgor pressure (Fig.3.13),

377 suggesting that the function of the scaffold is not to counter turgor pressure.

378

379 Scission efficiency decreases with decreased amounts of Rvs: in diploids, lowering the amount
380 of Rvs by 20 molecules decreases scission efficiency to about 90% from 97%. This indicates that
381 a particular coverage of the membrane tube is required for effective scaffolding by BAR domains.
382 In support of this, in BAR strains, fewer numbers of Rvs are recruited, and scission efficiency is
383 similarly reduced. At low concentrations of Rvs like in the 1xd cells, it is likely that some membrane
384 tubes recruit the critical number of Rvs, in which case the invaginations grow to near WT lengths.
385 Over a certain amount of Rvs, adding more BAR domains does not increase the stability of the
386 tube: in 4xd, the same amount of actin is recruited before scission as in the 2xd and 1xd strains. If
387 enough forces are generated at 80nm, why is scission efficiency decreased in *rvs167Δ* compared
388 to WT? Forces from actin may be at a threshold when the invagination is at 80nm. There could be
389 enough force to sever the membrane, but not enough to sever reliably. The Rvs scaffold then keeps
390 the network growing to accumulate enough actin to reliably cause scission. Controlling membrane
391 tube length could also be a way for the cell to control the size of the vesicles formed, and therefore
392 the amount of cargo packed into the vesicle.

393 **What causes membrane scission?**

394 We have tested several scission models that include a major role for the Rvs complex. The seemingly
395 obvious solution to the scission problem is the action of a dynamin-like GTPase. If loss of the yeast
396 Dynamin Vps1 prevented or delayed scission, the membrane would continue to invaginate longer
397 than WT lengths, and Sla1 movements of over 140nm should be observed. Rvs centroid movement
398 would likely also be affected: a bigger jump inwards could indicate that a longer membrane has
399 been cut. That neither is seen in the behaviour of coat and scission markers indicates that even if
400 Vps1 is recruited to endocytic sites, it is not necessary for Rvs localization or function, and is not
401 necessary for scission. The Inp51, Inp52 data tests the lipid hydrolysis model, in which synaptojanins
402 hydrolyze PIP2 molecules that are not covered by BAR domains, resulting in a boundary between
403 hydrolyzed and non- hydrolyzed PIP2. This model predicts that interfacial forces generated at the
404 lipid boundary causes scission (Liu et al., 2006). Inp51 is not seen in patches at the cellular cortex,
405 but this could be because protein recruitment is below our detection threshold. Inp52 localizes to
406 the top of invaginations right before scission, consistent with a role in vesicle formation (Fig.3.7D).
407 Some predictions of the lipid hydrolysis model are inconsistent with our data, however. First, vesicle
408 scission is expected to occur at the interphase of the hydrolyzed and non-hydrolyzed lipid. Since the
409 BAR scaffold covers the membrane tube, this interphase would be at the top of the area covered by
410 Rvs. Kukulski et al., 2012 have shown that vesicles undergo scission at 1/3 the invagination length
411 from the base: that is, vesicles generated by the lipid boundary would be smaller than have been
412 measured. Second, removing forces generated by lipid hydrolysis by deleting synaptojanins should
413 increase invagination lengths, since scission would be delayed or it would fail without those forces.
414 Deletion of neither Inp51 nor Inp52 changes the invagination lengths: Sla1 movement does not
415 increase. That the position of the vesicle formed is also unchanged compared to WT is indicated by
416 the similar magnitude of the jump into the cytoplasm of the Rvs centroid. There are some changes
417 in the synaptojanin deletion strains (Fig.3.8). In *inp51Δ* cells, Rvs assembly is slightly slower than
418 that in WT. Therefore, Inp51 could play a role in Rvs recruitment. In the *inp52Δ* strain, about 12% of
419 Sla1-GFP tracks retract, indicated that scission fails in those cases. Although this is low compared to
420 the failed scission rate of *rvs167Δ* cells (close to 30%), this data could suggest a moderate influence
421 of Inp52 on scission. Rvs centroid persists after scission for about a second longer in *inp52Δ* cells
422 than in WT, indicating that disassembly of Rvs on the base of the newly formed vesicle is delayed.
423 Inp52 is likely involved in vesicle un- coating Deletion of synaptojanin-like Inp52 does not affect the
424 movement of the invagination. In spite of this, Sla1 patches persist for longer after scission in the
425 *inp52Δ* than in WT cells, as does Rvs167, indicated by the arrows in Fig.3.8A,D. Persistence of both
426 suggests that rather than the scission timepoint, post-scission disassembly of proteins from the

vesicle is inhibited in *inp52Δ* cells. Inp52 then plays a role in recycling endocytic proteins from the vesicle to the plasma membrane. The slower assembly of Rvs in *inp51Δ* and the increase in coat retraction rates of *inp52Δ* could indicate that there is a slight effect on Rvs recruitment, and that lipid hydrolysis could play a small role in scission.

Protein-friction mediated membrane scission proposes that BAR domains induce a frictional force on the membrane, causing scission. In Rvs duplicated haploid cells (2xh), adding up to 1.6x the WT (1xh) amount of Rvs to membrane tubes does not affect the length at which the membrane undergoes scission (Fig.3.9). If more BAR domains were added to the membrane tube, frictional force generated as the membrane is pulled under it should increase, and the membrane should rupture faster. That is, membrane scission occurs as soon as WT forces are generated on the tube. Since BAR domains are added at a faster rate in the 2xh cells, these forces would be reached at shorter invagination lengths. In 2xh cells, WT amount of Rvs is recruited at about 1.8 seconds before maximum fluorescent intensity, but scission does not occur at this time. Instead, Rvs continues to accumulate, and the invagination continues to grow. In diploid strains, adding 1.4x the WT amount of Rvs in the 4x Rvs case also does not change length of membrane that undergoes scission. Therefore, protein friction due to Rvs does not appear to contribute significantly to membrane scission in yeast endocytosis.

Maximum amount of Abp1 measured in all the diploid strains is about 220 molecules (Fig.3.11). In this case, only one allele of Abp1 is fluorescently tagged, so half the amount of Abp1 recruited is measured. The maximum amount of Abp1 recruited is then double that measured, which is about 440 ± 20 molecules (assuming equal expression and recruitment of tagged and untagged Abp1). In WT haploid cells, the maximum number of Abp1 measured is 460 ± 20 molecules. That the same number of molecules of Abp1 is recruited in all cases before scission indicates that scission timing depends on the amount of Abp1, and hence, on the amount of actin recruited. This data is consistent with actin supplying the forces necessary for membrane scission. The membrane invagination continues until the "right" amount of actin is recruited. At this amount of actin, enough forces are generated to rupture the membrane. The amount of force necessary is determined by the physical properties of the membrane like membrane rigidity, tension, and proteins accumulated on the membrane (Dmitrieff and Needeelec, 2015). Vesicle scission releases membrane-bound Rvs, resulting in release of the SH3 along with BAR domains. Release of the SH3 domains could indicate to its binding partner in the actin network that vesicle scission has occurred, beginning disassembly of actin components. In BAR strains, a low amount of actin is recruited (Fig.3.4C). Although the absence of the SH3 domain severely perturbs the actin network, the mechanistic effect of this perturbation is unclear.

Model for membrane scission

I propose that Rvs is recruited to sites by two distinct mechanisms. SH3 domains cluster Rvs at endocytic sites. This SH3 interaction increases the efficiency with which the BAR domains sense curvature on tubular membranes. BAR domains bind to endocytic sites by sensing tubular membrane. BAR domains are recruited over the entire membrane tube, but do not form a tight helical scaffold. Membrane shape is stabilized against fluctuations that could cause scission by the BAR-membrane interaction. This prevent actin forces from rupturing the membrane, and the invaginations continue to grow in length as actin continues to polymerize. BAR recruitment to membrane tubes is restricted by the surface area of the tube: after a certain amount of Rvs, the excess interacts with endocytic sites via the SH3 domain. Adding over a certain amount of Rvs also does not increase the stabilization effect on the tube. As actin continues to polymerize, at a certain amount of actin, enough forces are generated to overcome the resistance to membrane scission provided by the BAR scaffold. The membrane ruptures, and vesicles are formed. Synaptojanins may help recruit Rvs at endocytic sites: Inp51 and Inp52 have proline rich regions that could act as binding sites for Rvs167 SH3 domains. They are involved in vesicle uncoating post-scission, likely by

dephosphorylating PIP2 and inducing disassembly of PIP2-binding endocytic proteins. Eventually phosphorylation regulation allows endocytic proteins to be reused at endocytic sites, while the vesicle is transported elsewhere into the cell.

Morbi luctus, wisi viverra faucibus pretium, nibh est placerat odio, nec commodo wisi enim eget quam. Quisque libero justo, consectetur a, feugiat vitae, porttitor eu, libero. Suspendisse sed mauris vitae elit sollicitudin malesuada. Maecenas ultricies eros sit amet ante. Ut venenatis velit. Maecenas sed mi eget dui varius euismod. Phasellus aliquet volutpat odio. Vestibulum ante ipsum primis in faucibus orci luctus et ultrices posuere cubilia Curae; Pellentesque sit amet pede ac sem eleifend consectetur. Nullam elementum, urna vel imperdiet sodales, elit ipsum pharetra ligula, ac pretium ante justo a nulla. Curabitur tristique arcu eu metus. Vestibulum lectus. Proin mauris. Proin eu nunc eu urna hendrerit faucibus. Aliquam auctor, pede consequat laoreet varius, eros tellus scelerisque quam, pellentesque hendrerit ipsum dolor sed augue. Nulla nec lacus.

Methods and Materials

Guidelines can be included for standard research article sections, such as this one.

Nulla malesuada porttitor diam. Donec felis erat, congue non, volutpat at, tincidunt tristique, libero. Vivamus viverra fermentum felis. Donec nonummy pellentesque ante. Phasellus adipiscing semper elit. Proin fermentum massa ac quam. Sed diam turpis, molestie vitae, placerat a, molestie nec, leo. Maecenas lacinia. Nam ipsum ligula, eleifend at, accumsan nec, suscipit a, ipsum. Morbi blandit ligula feugiat magna. Nunc eleifend consequat lorem. Sed lacinia nulla vitae enim. Pellentesque tincidunt purus vel magna. Integer non enim. Praesent euismod nunc eu purus. Donec bibendum quam in tellus. Nullam cursus pulvinar lectus. Donec et mi. Nam vulputate metus eu enim. Vestibulum pellentesque felis eu massa.

Citations

LaTeX formats citations and references automatically using the bibliography records in your .bib file, which you can edit via the project menu. Use the `\cite` command for an inline citation, like `?`, and the `\citep` command for a citation in parentheses (`?`). The LaTeX template uses a slightly-modified Vancouver bibliography style. If your manuscript is accepted, the eLife production team will re-format the references into the final published form. *It is not necessary to attempt to format the reference list yourself to mirror the final published form.* Please also remember to **delete the line** `\nocite{*}` in the template just before `\bibliography{...}`; otherwise *all* entries from your .bib file will be listed!

Acknowledgments

Additional information can be given in the template, such as to not include funder information in the acknowledgments section.